

PAPER • OPEN ACCESS

Low-energy beam transport system for MESA

To cite this article: C. Matejcek *et al* 2019 *J. Phys.: Conf. Ser.* **1350** 012027

View the [article online](#) for updates and enhancements.



IOP | ebooks™

Bringing you innovative digital publishing with leading voices to create your essential collection of books in STEM research.

Start exploring the **collection** - download the first chapter of every title for free.

Low-energy beam transport system for MESA

C. Matejcek¹, K. Aulenbacher^{1,2,3} and S. Friederich¹

¹Institut für Kernphysik, Johannes Gutenberg-Universität Mainz, Germany

²Helmholtz Institut Mainz, Germany

³GSI Helmholtzzentrum für Schwerionenforschung, Darmstadt, Germany

E-mail: matejcek@uni-mainz.de

Abstract. An important part of the new accelerator MESA (Mainz Energy-recovering Superconducting Accelerator) is the low-energy beam transport system connecting the 100 keV electron source with the injector. The present setup includes the chopper and bunching system. The devices are of highest importance in order to achieve sufficient bunch compression, particularly at higher bunch charges and currents. With the circularly deflecting cavity of the chopper system it is possible to measure the longitudinal profile of the bunches upstream of the buncher, whereas downstream the longitudinal size will be measured by Smith-Purcell radiation. Based on experimental results obtained from this setup, we will discuss the beam parameters and compare them with simulations of the beamline.

1. Introduction

The MESA accelerator will serve for particle physics experiments, in particular the P2 experiment [1] and the MAGIX experiment [2]. Both make different demands on the accelerator. While P2 requires high beam availability and a spin polarized beam, MAGIX asks for high beam currents. For this reason, the interface MELBA (MESA Low-energy Beam Apparatus) between the spin-polarized photosource [3] and the MESA injector must be capable of spin manipulation, transverse and longitudinal matching, and transport of high currents. With the very clean beam that can be obtained from a chopper/buncher system that is a scaled version of the proven MAMI system [4,5,6], MELBA is certainly well adapted to the needs of the P2 experiment that operates at a current of 150 μ A. The current operating voltage of the source is 100 kV, which is relatively low to provide safe operational conditions for the very sensitive GaAs photocathodes, which enable spin polarization but do not tolerate field emission. Transporting the beam at a low energy facilitates spin manipulation [7] but is a disadvantage concerning high currents because of space charge forces. In addition, the beamline is very long due to the installation of the devices mentioned above. Therefore it is not evident that the bunch charges of in the order of 1 pC demanded by MAGIX can be transported and matched through MELBA. The main purpose of our investigations is if the MELBA setup can satisfy the requirements of both experiments; otherwise, a dedicated source with higher acceleration voltage and shorter injection system would become mandatory.

2. Experimental setup

Figure 1 shows the most relevant components for this investigation of the lattice. Two different laser setups were used. The first one is a single-mode laser with an elliptical spot size of



Content from this work may be used under the terms of the [Creative Commons Attribution 3.0 licence](https://creativecommons.org/licenses/by/3.0/). Any further distribution of this work must maintain attribution to the author(s) and the title of the work, journal citation and DOI.

$\sigma_x = 144 \mu\text{m}$ and $\sigma_y = 285 \mu\text{m}$ and a wavelength of 802 nm. The disadvantage of this laser system is that it is limited to an output power of 25 mW, so that it is not possible to reach very high currents with a typical photosensitivity of a few mA/W. The laser diode is driven by a pulse generator. For the presented investigations, a duty cycle of 1/4 and a pulselength of 100 μs , which corresponds to 13000 rf periods, are used. Considering the beam dynamics, this is equivalent to a dc current. The second laser is a fibre-coupled multi-mode diode with a wavelength of 808 nm, an elliptical spot size of $\sigma_x = 560 \mu\text{m}$ and $\sigma_y = 780 \mu\text{m}$ and a maximum output power of 5 W. For currents up to 10 μA , the dc mode was used, whereas for higher currents, 260 μs pulses with an increasing duty cycle up to 1/200 were used, which is also equivalent to a dc current. This is necessary for photocathode lifetime reasons and to prevent damaging the diagnostic devices. Both lasers allow to produce a spin-polarized beam.

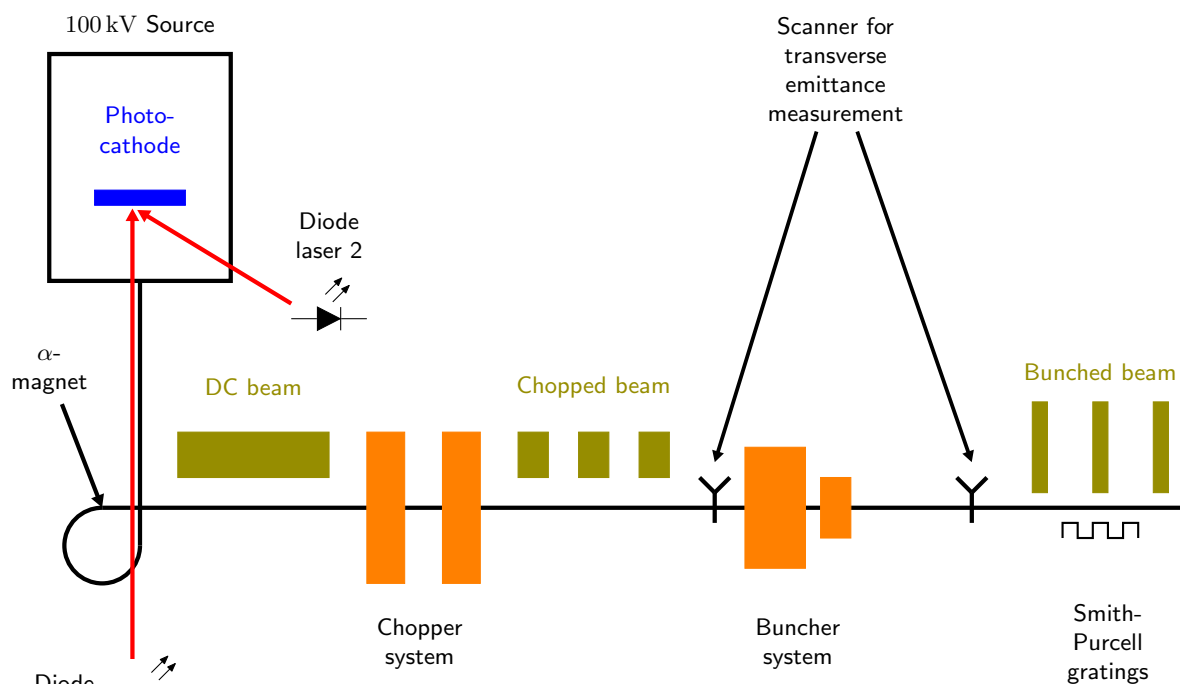


Figure 1. Scheme of the test setup.

The idea of diode laser 1 was to have a beam with good quality as the smaller emitting area leads to a smaller initial emittance of the electron beam. Therefore, it is useful to investigate finer details of beam-dynamics, like the small absolute emittance growth induced by mis-tuning of the chopper system. The electrons extracted from a photocathode in the source are focused by quadrupoles and solenoids. The beam is bent by 270° by an alpha magnet. Several steerers are employed to compensate for stray magnetic fields. All beam guidance is omitted in Fig. 1 for a better overview. For offline characterisation of the beam, several scanners are installed. The presented emittance measurements were done with a tungsten wire of 30 μm in diameter. The wire is continuously moved along the beam, which results in the fraction of the beam which hits the wire producing X-rays. These are detected and integrated by a scintillator/PMT combination that is followed by suitable electronics. The amount of data points along the beam depends on the velocity of the wire and the duty cycle. This is done for several focussing strengths of a solenoid, and the emittance is reconstructed by the standard procedure described in [8]. The most complex part is the chopper and buncher system responsible for matching

the beam with the longitudinal acceptance of the injector. The chopper system consists of two circularly deflecting cavities with a resonance frequency of 1.3 GHz, a solenoid, and a collimator. For longitudinal bunching, also two cavities are used, the first one with a resonance frequency of

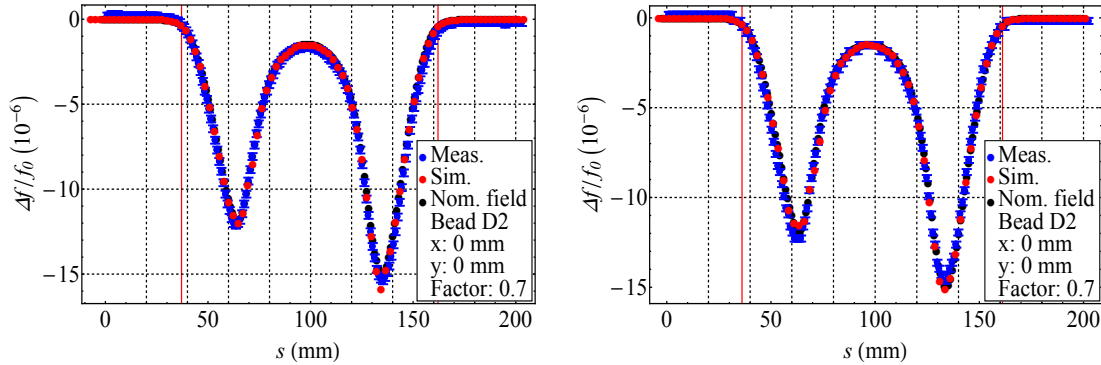


Figure 2. Measurements and simulations of the electric field on the reference axis in the chopper cavities.

1.3 GHz and the second one with double the frequency. This is necessary to get a linear velocity modulation along the bunch [6]. To measure the longitudinal dimension behind the buncher a Smith-Purcell radiation (SPR) [9] chamber is installed so that the operation principle of the buncher can be verified. However, we will not discuss these results here.

3. Measurements

3.1. Chopper system

The chopper system consists of two circularly deflecting cavities, a double solenoid [10], and a collimator [11]. Only a fractional part of the circle passes the collimator, turning the dc beam into a cw beam with a frequency of 1.3 GHz. The gap of the collimator can be varied, and with it the bunchlength of the beam. The solenoid images the beam from the first cavity to the second one. Therefore, the transverse deflection of the first cavity can be compensated for the same deflection of the second cavity. To achieve this, the amplitude of the double solenoid and the phase of the second cavity with respect to the first one have to be adjusted. After brazing the chopper cavities, a last field measurement was done (see Fig. 2). The measured field agrees with the nominal field. The final parameters with adjusted input and output antennas are $f = 1.3$ GHz, coupling $\kappa = 1$, Smith parameter $S_{11} = -50$ dB and $S_{21} = -30$ dB. A wrong adjustment of the solenoid field leads to an emittance growth in the horizontal plane, whereas a wrong rf phase of the second cavity leads to a higher emittance in the vertical plane. Therefore, the ideal operating point can be found by minimizing the emittance in both planes. The corresponding measurements are shown in Fig. 3. Even with optimal parameters, turning on the chopper system leads to an emittance growth as Fig. 4 depicts. The same behavior is observed with the buncher cavities, which is illustrated in Fig. 5 for the cavity with 1.3 GHz. About 60% of the beam is dumped at the chopper collimator. The additional growth of the emittance with increasing input power, which corresponds to focussing strength of the buncher, is induced by the longitudinal compression. Thereby the defocussing space charge force in the transverse direction is enlarged especially at higher beam currents as it is shown. This also indirectly proves the functionality of the buncher cavity.

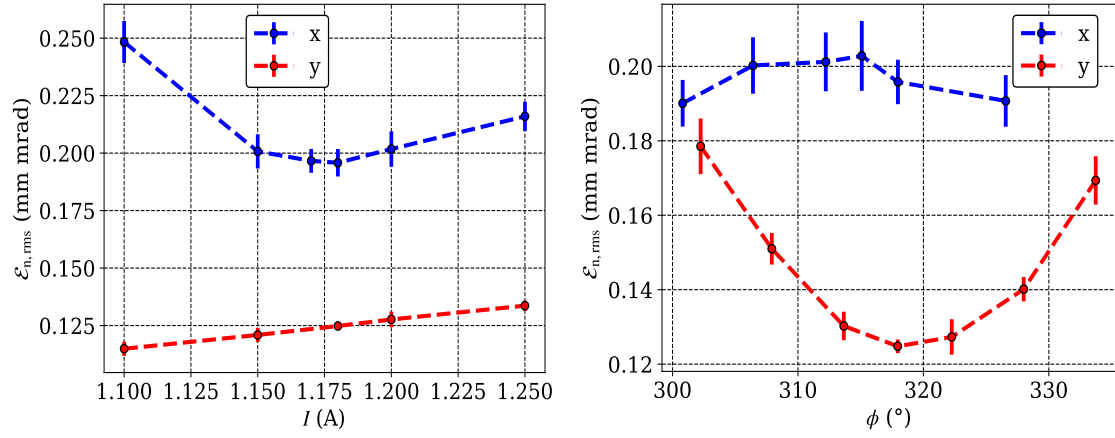


Figure 3. Emittance growth due to wrong magnetic field of the double solenoid (left) and wrong rf phase of the second chopper cavity.

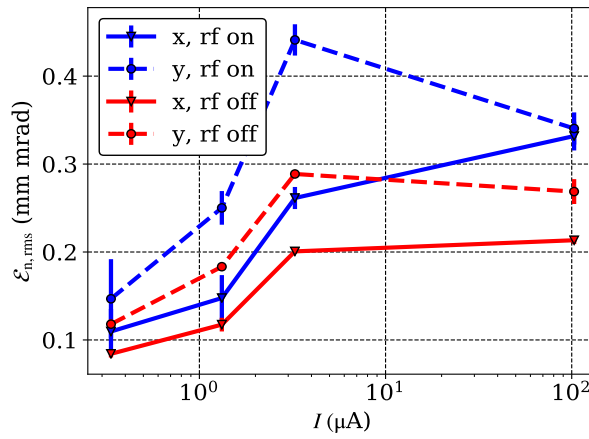


Figure 4. Emittance growth due to chopper system for different beam currents.

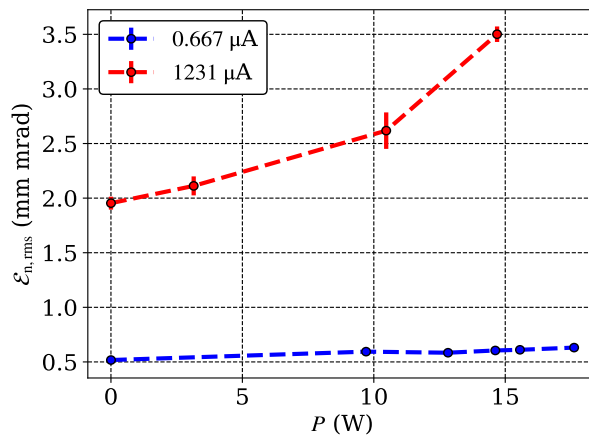


Figure 5. Emittance growth due to turning on and increasing the power of the buncher system for two beam currents.

3.2. High-Current Emittance Measurements

The presented emittance measurements were done with the last scanner so the distance travelled by the electrons is 5 m. Figure 6 presents the results. In contrast to the chopper system, the buncher system was not used here. First the current was measured at the source and at the

beamdump without the chopper system. It was possible to reach a transmission of over 99 %. One has to consider that the currents in Fig. 6 are measured in front of the chopper system where around 60 % of the beam is dumped. The blue (middle) data points are the measurements with the diode laser 1 and in red (top) the measurements with the second laser system. As mentioned above, the laser spot of the first one is about a factor 3 smaller than the second one. This is the reason for the difference of the emittances in Fig. 6. In both cases, the emittance begins to increase considerably around a beam current of 100 μA . The green (bottom) data points

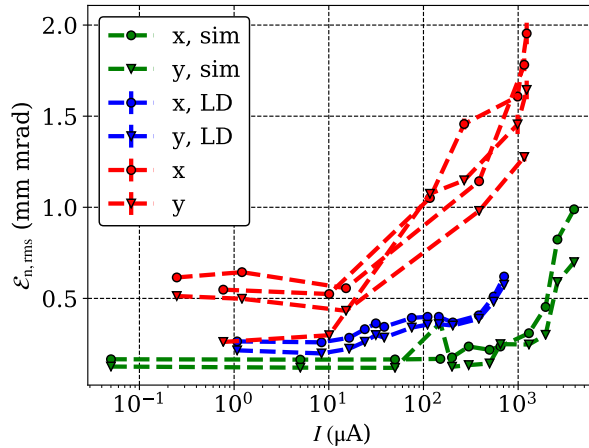


Figure 6. Emittance measurements and simulations for different beam currents.

represent simulations of the beamline done with a combination of the two particle dynamics codes PARMELA [12] and CST [13]. Here, the emittance starts to increase at currents of an order of magnitude higher. Reasons for this discrepancy could be fringe fields of the magnets and nonlinear magnetic field components. Furthermore, it is not possible to shield the whole magnetic field of the earth, which also disturbs the beam. In addition to that, misalignment of devices could play a role. The influence of these issues has to be investigated further to improve the emittance of high current beams.

4. Summary and outlook

A 6.5 m long test beamline was built successfully, including the adjustment of the chopper system. The diagnostic devices allow measurements of the emittance in both transverse planes. First measurements were done and show a discrepancy with the simulations of the beamline. Here, both measurements and simulations have to be checked to explain the difference. However, it is possible to transport the beam currents of polarized electrons demanded by the experiments. Additionally, the emittance measurements with a running buncher system have to be done in the whole possible beam current range.

Acknowledgments

Acknowledgement This work is supported by the DFG excellence initiative PRISMA+, within the GRK 2128 and by the German Federal Ministry of Education and Research within Verbundforschungsprojekt HOPE-2, FKZ 05K16UMA.

References

- [1] Becker D *et al.* 2018 The p2 experiment *arXiv* doi:10.1140/epja/i2018-12611-6
- [2] Doria L, Achenbach P, Christmann M, Denig A, Gülker P and Merkel H 2018 Search for light dark matter with the MESA accelerator *13th Conf. on the Intersections of Particle and Nuclear Physics (CIPANP 2018)*

- [3] Friederich S, Matejcek C and Aulenbacher K 2019 Vacuum lifetime and surface charge limit investigations concerning high intensity spin-polarized photoinjectors *10th Int. Particle Accelerator Conf. (IPAC'19)*, Melbourne, Australia, paper TUPTS011, this conference.
- [4] Braun H H 1988 Das Choppersystem für den Injektorlinac des Mainzer Mikrotrons, Diploma thesis, Phys. Dept., Institut für Kernphysik, Mainz, Germany
- [5] Bechthold V 2013 Eine Deflektor-Kavität für den MESA-Beschleuniger, Diploma thesis, Phys. Dept., Institut für Kernphysik, Mainz, Germany
- [6] Heil P 2015 Longitudinale Emittanzanpassung durch Geschwindigkeitsmodulation im Injektionssystem an MESA, Master thesis, Phys. Dept., Institut für Kernphysik, Mainz, Germany
- [7] Tioukine V and Aulenbacher K 2006 Operation of the MAMI accelerator with a Wien filter based spin rotation system *Nuclear Instruments and Methods in Physics Research Section A: Accelerators, Spectrometers, Detectors and Associated Equipment* **568** pp. 537–42
- [8] Alexander I 2018 Experimental investigation of the beam dynamics of the MESA photoinjector, Ph.D. thesis, Phys. Dept., Institut für Kernphysik Mainz Germany
- [9] Heil P and Aulenbacher K 2018 Smith-Purcell Radiation for Bunch Length Measurements at the Injection of MESA *Proc. IPAC18* Vancouver BC Canada pp. 4213–15, doi:10.18429/JACoW-IPAC2018-THPMF062
- [10] Stoll C 2016 Solenoid-Fokussierungsmagnete für den niederenergetischen Strahltransport an MESA, Master thesis, Phys. Dept., Institut für Kernphysik, Mainz, Germany
- [11] Ledroit B 2016 Aufbau und Test des MESA-Choppers, Master thesis, Phys. Dept., Institut für Kernphysik, Mainz, Germany
- [12] PARMELA, Phase and radial motion in electron linear accelerators, 2005
- [13] CST STUDIO SUITE 2016, Computer simulation technology